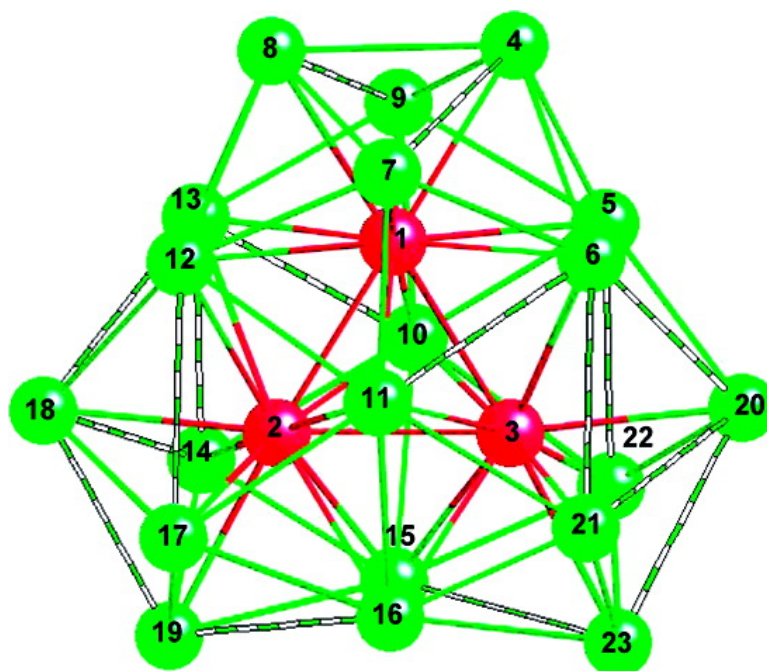Article

Nanosized Pd(CO){P(*p*-Tolyl)} Containing Geometrically Unprecedented Central 23-Atom Interpenetrating Tri-icosahedral Palladium Kernel of Double Icosahedral Units: Its Postulated Metal-Core Evolution and Resulting Stereochemical Implications

Evgueni G. Mednikov, and Lawrence F. Dahl

More About This Article

Additional resources and features associated with this article are available within the HTML version:

- Supporting Information
- Access to high resolution figures
- Links to articles and content related to this article
- Copyright permission to reproduce figures and/or text from this article

ACS Publications
High quality. High impact.

View the Full Text HTML

Nanosized Pd$_{37}$(CO)$_{28}${P(p-Tolyl)$_3$}$_{12}$ Containing Geometrically Unprecedented Central 23-Atom Interpenetrating Tri-icosahedral Palladium Kernel of Double Icosahedral Units: Its Postulated Metal-Core Evolution and Resulting Stereochemical Implications

Evgueni G. Mednikov* and Lawrence F. Dahl*

Department of Chemistry, University of Wisconsin—Madison, Madison, Wisconsin 53706

Received July 21, 2008; E-mail: mednikov@chem.wisc.edu; dahl@chem.wisc.edu

Abstract: Pd$_{37}$(CO)$_{28}${P(p-Tolyl)$_3$}$_{12}$ (**1**) was obtained in ~50% yield by the short-time thermolysis of Pd$_{10}$(CO)$_{12}${P(p-Tolyl)$_3$}$_6$ in THF solution followed by crystallization via layering with hexane under N$_2$. The low-temperature (100 K) CCD X-ray diffraction study of **1** revealed an unusual non-spheroidal Pd$_{37}$-atom polyhedron, which may be readily envisioned to originate via the initial formation of a heretofore non-isolated central Pd$_{23}$ kernel composed of three interpenetrating trigonal-planar double icosahedra (DI) that are oriented along the three bonding edges of its interior Pd$_3$ triangle. This central Pd$_{23}$ kernel is augmented by face condensations with two additional phosphorus-free and 12 tri(p-C$_6$H$_4$Me)phosphine-ligated Pd atoms, which lower the pseudo-symmetry of the resulting 37-atom metal core from D_{3h} to C_2. The 12 P atoms and 28 bridging CO connectivities preserve the *pseudo-C$_2$* symmetry. The central Pd$_{23}$ kernel in **1** provides the only crystallographic example of the 23-atom member of the double icosahedral family of "twinned" interpenetrating icosahedra (II), which includes the 19-atom two II (1 DI), the 23-atom three II (3 DI), the 26-atom four II (6 DI), and the 29-atom five II (9 DI). The n-atoms of these DI models coincide exactly with prominent atom-peak maxima of 19, 23, 26, and 29, respectively, in the mass spectrum of charged argon clusters formed in a low-temperature free-jet expansion. The only previous crystallographically proven 26- and 29-atom DI members are the central *pseudo-T$_d$* tetrahedral Pd$_{26}$ kernel (4 II, 6 DI) in the PMe$_3$-ligated Pd$_{29}$Ni$_3$(CO)$_{22}$(PMe$_3$)$_{13}$ (**2**) and the central *pseudo-D$_{3h}$* trigonal-bipyramidal Pd$_{29}$ kernel (5 II, 9 DI) in the PMe$_3$-ligated Pd$_{35}$(CO)$_{23}$(PMe$_3$)$_{15}$ (**3**). Two highly important major stereochemical implications are noted: (1) The formation of geometrically identical idealized architectures for these three II palladium kernels with corresponding DI models constructed for the charged argon clusters provides compelling evidence that the nature of delocalized Pd–Pd bonding in these II (and presumably other nanosized) Pd clusters, in which each zerovalent Pd atom individually has a closed-subshell 4d^{10} ground state, may likewise (as in argon clusters) be viewed primarily in terms of (considerably stronger) *attractive dispersion interactions*. (2) The existence of the 23-atom II Pd$_{23}$ kernel in **1** provides an essential heretofore "missing" geometrical link as an intermediate in the same sequential growth pathway to give the 26- and 29-atom II Pd$_n$ kernels found in **2** and **3**, respectively. Accommodation of the 12 bulky P(p-Tolyl)$_3$ ligands around the entire 37-atom palladium core necessitates an extended metal surface that originates from the *pseudo*-2D trigonal-planar Pd$_{23}$ kernel found in **1**. The much smaller PMe$_3$ ligands in **2** and **3** would sterically allow further sequential transformations of an initially formed 23-atom II intermediate palladium kernel into the 26-atom *spheroidal* II palladium kernel in **2** or further into the 29-atom *semi-spheroidal* II palladium kernel in **3**, but with smaller total metal-atom nuclearities of 32 and 35, respectively.

Introduction

Our combined research over three decades has shown that palladium functions as a unique transition metal in forming an astonishingly broad, unparalleled family of nanosized CO/PR$_3$-ligated homopalladium clusters (i.e., ones with metal cores comprising at least 10 metal atoms that are involved in direct metal–metal bonding).[1,2] Prior to the cluster reported herein, these highly condensed metal clusters were ascertained from X-ray crystallographic studies[2] to possess 18 distinctly different homopalladium architectures; all but three of those clusters[2] were found to contain central close-packed metal fragments (denoted herein as kernels) with structural units that may be described as cubic close-packed (ccp) or mixed ccp/hexagonal close-packed (hcp) stacking layers (with sequences corresponding to truncated or capped octahedra and to centered cuboctahedra or anticuboctahedra) and as single icosahedra or face-fused polyicosahedra. One exception is the Pd$_{38}$ cluster that has a highly irregular core geometry,[3a] while the second exception is one of two highly dissimilar (but reversibly interconvertible) Pd$_{23}$ clusters[4] that has a highly distorted body-centered cubic (bcc) core-framework.[3b] The close-packed structural units also include "twinned" interpenetrating cuboctahedral and interpenetrating icosahedral (*vide infra*) frameworks along with one mixed face-fused octahedral/icosahedral Pd$_{59}$ architecture con-

sisting of a central bioctahedron that trans-caps two centered icosahedra.[5] The third exception is the largest crystallographically determined homopalladium cluster that completely differs from the others in containing a concentric capped three-shell 145-atom metal core of pseudo-I_h symmetry.[6]

One especially notable stereochemical feature of this extraordinary family of $[Pd_n(CO)_x(PR_3)_y]$ clusters is that the majority of the clusters were prepared with the triethylphosphine ligand,[7] which is sterically non-bulky (Tolman[8] cone angle, 132°) and a good σ-electron donor. In fact, the above-reported Pd_n clusters (to date) *not* possessing PEt_3 ligation are the Pd_{12} cluster that was isolated only with PPh_3 or $P(n\text{-}Bu)_3$ ligands[9] and the Pd_{35}, Pd_{39}, and Pd_{59} clusters[5] that were obtained only with the sterically smaller PMe_3 ligand (Tolman[8] cone angle, 118°). Furthermore, it was shown that all of the PEt_3-containing homopalladium clusters could be obtained from reactions involving the same tetra(edge-capped) octahedral Pd_{10} parent precursor, $Pd_{10}(CO)_{12}(PEt_3)_6$,[10] through different kinetically controlled synthetic routes. For most of these clusters, reasonably good yields (at least 30%) were ultimately achieved by optimization of the reaction conditions and, in several cases,

by the structure-to-synthesis approach involving the designed use of different structurally suggested synthetic pathways.

Our previous choice of trimethylphosphine as a reactant,[5] which successfully gave rise to the new Pd_n clusters ($n = 35$, 39, 59), was based upon the premise that smaller PMe_3 ligands would likely play a crucial steric role in obtaining nanosized palladium clusters with larger metal-core sizes. Although this long-standing experimentally observed view that stabilization of high-nuclearity metal clusters requires small ligands is generally followed,[11] it was shown *not* to be the case in the unexpected recent preparation and crystallographic/magnetic characterization of the remarkable PPh_3-ligated Pt-centered "full" four-shell 165-atom Pd–Pt cluster, $(\mu_{12}\text{-Pt})Pd_{164-x}\text{-}Pt_x(CO)_{72}(PPh_3)_{20}$ ($x \sim 7$),[2] which is the largest reported crystallographically determined discrete transition metal cluster (to date) with direct metal–metal bonding. However, a comparative analysis[2] with the geometrically related $Pd_{145}(CO)_x(PEt_3)_{30}$ ($x \sim 60$)[6] revealed that the 10 fewer PR_3 ligands in the 165-atom Pd–Pt cluster versus the PEt_3-ligated Pd_{145} cluster necessitate the larger bulky PPh_3 ligands (Tolman[8] cone angle, 145°) in order to protect the Pd–Pt core-geometry. As part of current efforts to increase both its yield ($<10\%$) and solubility in order to perform extensive physical studies including multi-nuclear NMR/electrochemical measurements, the corresponding $Pd_{10}(CO)_{12}\{P(p\text{-Tolyl})_3\}_6$[12] analogue (**4**)[12] of the $Pd_{10}(CO)_{12}\text{-}(PPh_3)_6$ precursor[12] of the Pd–Pt cluster is being used in reactions with both zerovalent Pt and Pd reagents.

Herein we present the resulting thermolysis reaction of this analogue (**4**) possessing $P(p\text{-}C_6H_4Me)_3$ ligands (same Tolman[8] cone angle, 145°) in THF, which has produced unexpectedly, in good yield (56%), the nanosized $Pd_{37}(CO)_{28}\{P(p\text{-Tolyl})_3\}_{12}$ (**1**) containing the Pd_{23} kernel that corresponds to a heretofore "missing" key tri-icosahedral palladium member of the double-icosahedral (DI) family of "twinned" interpenetrating icosahedra (**II**).[13] The only other crystallographically established 26- and 29-atom DI members are the central 26-atom II Pd_{26} kernel in $Pd_{29}Ni_3(CO)_{22}(PMe_3)_{13}$ (**2**)[5] and the central 29-atom II Pd_{29} kernel in $Pd_{35}(CO)_{23}P(Me_3)_{15}$ (**3**).[5] The Pd_{26} kernel consists of four II (formed from six 19-atom DI), with the four icosahedrally centered interior Pd(i) atoms arranged in a strongly bonding $Pd(i)_4$ tetrahedron that is encapsulated by 22 Pd(cage) atoms; the Pd_{29} kernel is composed of five II (formed from nine DI) with the five icosahedrally centered interior Pd(i) atoms geometrically possessing a bonding $Pd(i)_5$ trigonal bipyramid that is surrounded by 24 Pd(cage) atoms. These three ligated II Pd_n kernels ($n = 23, 26, 29$) are considered herein to originate via the same sequential growth pathway (with the Pd_{23} kernel in **1** then being an intermediate), as was originally proposed[13b] for the atomic growth sequence of prominent *n*-atom argon clusters ($n = 19, 23, 26, 29$) that were observed in the mass spectrum of charged argon clusters generated in a low-temperature free-jet expansion.[14]

Highly significant general implications based upon this direct analogy of identical II geometries are presented. This research thereby has prime structural/bonding relevance in connection with larger non-crystalline naked/ligated nanoparticles and hence

(1) For reviews, see: (a) Femoni, C.; Iapalucci, M. C.; Kaswalder, F.; Longoni, G.; Zacchini, S. *Coord. Chem. Rev.* **2006**, *250*, 1580. (b) Belyakov, O. A.; Slovokhotov, Yu. L. *Russ. Chem. Bull.* **2003**, *52*, 2299 (Engl. transl.). (c) Collini, D.; Femoni, C.; Iapalucci, M. C.; Longoni, G.; Zanello, P. In *Perspectives in Organometallic Chemistry*; Screttas, C. G., Steele, B. R., Eds.; Special Publication No. *287*; Royal Society of Chemistry: London, 2003; p 183. (d) Stromnova, T. A.; Moiseev, I. I. *Usp. Khim.* **1998**, *67*, 542; *Russ. Chem. Rev.* **1998**, *67*, 485 (Engl. transl.). (e) Longoni, G.; Iapalucci, M. C. In *Clusters and Colloids: From Theory to Applications*; Schmid, G., Ed.; VCH Publ. Inc.: New York, NY, 1994; pp 91–177. (f) Ceriotti, A.; Pergola, R. D.; Garlaschelli, L. In *Physics and Chemistry of Metal Cluster Compounds*; de Jongh, L. J., Ed.; Kluwer Academic Publ.: The Netherlands, 1994; Chapter 2, pp 41–106. (g) Burrows, A. D.; Mingos, D. M. P. *Transition Met. Chem.* **1993**, *18*, 129. (h) King, R. B. *Gazz. Chim. Ital.* **1992**, *122*, 383. (i) Eremenko, N. K.; Gubin, S. P. *Pure Appl. Chem.* **1990**, *62*, 1179. (j) Kharas, K. C. C.; Dahl, L. F. *Adv. Chem. Phys.* **1988**, *70*, 1 (Part 2). (k) Eremenko, N. K.; Mednikov, E. G.; Kurasov, S. S. *Usp. Khim.* **1985**, *54*, 671; *Russ. Chem. Rev.* **1985**, *54*, 394 (Engl. transl.).

(2) For a comprehensive listing of the nanosized palladium carbonyl phosphine clusters with different Pd_n core geometries (with $n \geq 10$), see: Mednikov, E. G.; Jewell, M. C.; Dahl, L. F. *J. Am. Chem. Soc.* **2007**, *129*, 11619.

(3) (a) Mednikov, E. G.; Eremenko, N. K.; Slovokhotov; Yu. L.; Struchkov, Yu. T. *J. Chem. Soc., Chem. Commun.* **1987**, 218. (b) Mednikov, E. G.; Eremenko, N. K.; Slovokhotov, Yu. L.; Struchkov, Yu. T. *Zh. Vsesoyuzn. Khim. Obs. Mendeleeva (Russ. J. Mendeleev's Chem. Soc.)* **1987**, *32*, 101.

(4) (a) Mednikov, E. G.; Wittayakun, J.; Dahl, L. F. *J. Cluster Sci.* **2005**, *16*, 429. (b) Mednikov, E. G.; Ivanov, S. A.; Wittayakun, J.; Dahl, L. F. *J. Chem. Soc., Dalton Trans.* **2003**, 1686.

(5) Tran, N. T.; Kawano, M.; Dahl, L. F. *J. Chem. Soc., Dalton Trans.* **2001**, 2731.

(6) Tran, N. T.; Powell, D. R.; Dahl, L. F. *Angew. Chem., Int. Ed.* **2000**, *39*, 4121.

(7) Mednikov, E. G.; Ivanov, S. A.; Slovokhotova, I. V.; Dahl, L. F. *Angew. Chem., Int. Ed.* **2005**, *44*, 6848.

(8) Tolman, C. A. *Chem. Rev.* **1977**, *77*, 313.

(9) (a) Mednikov, E. G.; Struchkov, Yu. T.; Slovokhotov, Yu. L. *J. Organomet. Chem.* **1998**, *566*, 15. (b) Kawano, M.; Bacon, J. W.; Campana, C. F.; Winger, B. E.; Dudeck, J. D.; Sirchio, S. A.; Scruggs, S. L.; Geiser, U.; Dahl, L. F. *Inorg. Chem.* **2001**, *40*, 2554 (see especially "Note Added in Proof" concerning the following reference). (c) Mednikov, E. G.; Eremenko, N. K.; Khivintseva, G. A. *Koord. Khim. (Sov. J. Coord. Chem.)* **1987**, *13*, 106.

(10) (a) Mednikov, E. G.; Eremenko, N. K.; Mikhailov, V. A.; Gubin, S. P.; Slovokhotov, Yu. L.; Struchkov, Yu. T. *J. Chem. Soc., Chem. Commun.* **1981**, 989. (b) Mednikov, E. G.; Eremenko, N. K.; Gubin, S. P.; Slovokhotov, Yu. L.; Struchkov, Yu. T. *J. Organomet. Chem.* **1982**, *239*, 401. (c) Mingos, D. M. P.; Hill, C. M. *Croat. Chem. Acta* **1995**, *68*, 745.

(11) Chini, P. *J. Organomet. Chem.* **1980**, *200*, 37.

(12) Mednikov, E. G.; Eremenko, N. K.; Gubin, S. P. *Koord. Khim. (Sov. J. Coord. Chem.)* **1984**, *10*, 711.

(13) (a) Farges, J.; de Feraudy, M. F.; Raoult, B.; Torchet, G. *Surf. Sci.* **1985**, *156*, 370. (b) Farges, J.; de Feraudy, M. F.; Raoult, B.; Torchet, G. *Adv. Chem. Phys.* **1988**, *70*, 45.

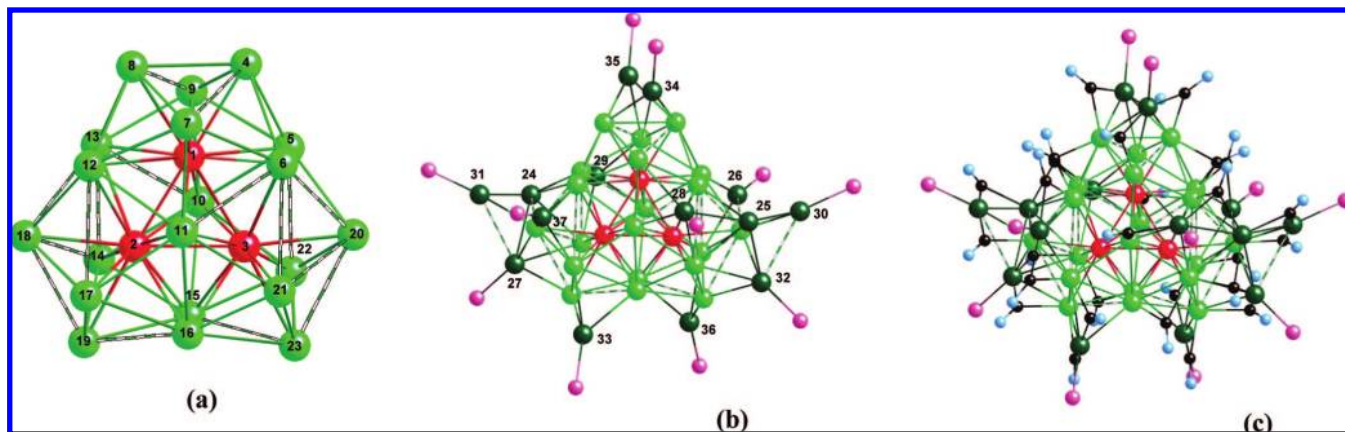(14) Harris, I. A.; Kidwell, R. S.; Northby, J. A. *Phys. Rev. Lett.* **1984**, *53*, 2390.

Figure 1. Anatomy of the solid-state structure of $Pd_{37}(CO)_{28}\{P(p\text{-}C_6H_4Me)_3\}_{12}$ (**1**). Its highly non-spheroidal geometry is envisioned to originate from the combined formal construction of: (1) a central interpenetrating tri-icosahedral Pd_{23} kernel that consists of a *pseudo-D_{3h}* framework formed from three DI, and (2) markedly asymmetrical face condensations with the 14 additional palladium atoms, which (along with 12 bulky terminal $P(p\text{-}C_6H_4Me)_3$ and 28 bridging carbonyl ligands) lower the *pseudo*-symmetry from D_{3h} (for the idealized Pd_{23} kernel) to C_2 for the entire cluster (upon exclusion of the P-attached tolyl substituents). (a) View of the central tri-icosahedral Pd_{23} kernel ($n = 1-23$) along the principal *pseudo*-three-fold axis passing through Pd(10), Pd(11), and with the molecular horizontal *pseudo-C_2* axis that passes through Pd(1) oriented vertically. The close resemblance of its *pseudo*-trigonal-planar architecture, formally constructed from three 19-atom DI that are oriented along the bonding edges of its interior $Pd(i)_3$ triangle, to *pseudo-D_{3h}* symmetry is apparent. Nevertheless, the Pd_{23} kernel itself exhibits a pronounced C_2-distorted architecture, as reflected from an examination of its Pd(cage)−Pd(cage) connectivities; this significant distortion from an idealized D_{3h} geometry is readily ascribed to the lower *pseudo-C_2* symmetry of the capping palladium atoms. The three Pd(n) atoms ($n = 1-3$) of the interior $Pd(i)_3$ triangle are colored red; the other 20 kernel Pd(n) atoms ($n = 4-23$), denoted as Pd(cage) atoms, are colored in light green. The horizontal σ_h mirror plane contains nine Pd(n) atoms ($n = 1, 2, 3, 4, 8, 18, 19, 20, 23$) comprised of the three interior triangular Pd(i) atoms and the three outermost apical Pd(cage) atoms of the three interpenetrating 19-atom DI. The other 14 Pd(cage) atoms in the Pd_{23} kernel are related in pairs by the σ_h mirror plane. (b) Same view, displaying the 37 palladium atoms and 12 P atoms of the $P(p\text{-}C_6H_4Me)_3$ ligands. The additional 14 dark-green colored Pd(n) atoms ($n = 24-37$), consisting of two phosphorus-free Pd(j) atoms ($n = 24, 25$) and 12 $P(p\text{-}C_6H_4Me)_3$-ligated Pd(cap) atoms ($n = 26-37$), form highly asymmetrical face condensations onto the *pseudo*-trigonal-planar Pd_{23} kernel; the resulting extended metal surface is needed to accommodate the 12 bulky Pd(cap)-attached $P(p\text{-}C_6H_4Me)_3$ ligands. Weakly bonding Pd−Pd connectivities with lengths greater than 3.0 Å are drawn in multi-band style. (c) Same view, showing the entire molecular structure of **1** with the phosphine tolyl substituents omitted for clarity. The C and O atoms of the 28 bridging C(n)O(n) carbonyls are shown in black and blue, respectively; two doubly bridging ones ($n = 4, 21$) and two triply bridging ones ($n = 7, 11$) are each coordinated exclusively to the II Pd_{23} kernel.

should be of particular interest to scientists in nanoscience and nanotechnology.

Results and Discussion

Molecular Configuration of 1. a. General Comments. An examination of the geometry of **1** reveals the remarkable anatomy described in Figure 1. Although **1** has no crystallographically imposed symmetry, its geometry (upon omission of the *p*-Tolyl substituents) ideally possesses a molecular two-fold axis. Mean distances and corresponding ranges of individual distances under *pseudo-C_2* symmetry are given in Table 1.

b. Metal-Core Geometry of 1 and Comparison of Structural Features with Other Interpenetrating Icosahedral Clusters. The configuration of this 37-atom palladium core is best described in terms of a central interpenetrating tri-icosahedral Pd_{23} kernel that is face-condensed by the other 14 palladium atoms. The 23-atom kernel has an interpenetrating *pseudo*-trigonal-planar tri-icosahedral framework that is composed of three 19-atom double icosahedra (DI) that are oriented along the bonding edges of a $Pd(i)_3$ triangle formed by the three interior Pd(i) atoms (colored red in Figure 1) located at the centers of three icosahedra. Each Pd(i) is thereby radially coordinated to the other two Pd(i) and 10 Pd(cage) atoms (colored light green) that form an individual icosahedron. The idealized geometry of this Pd_{23} kernel of three Pd(i) and 20 Pd(cage) atoms conforms to the D_{3h} point group, which consists of a principal C_3 axis (and a coincident S_3 axis), three horizontal C_2 axes, one horizontal σ_h mirror plane, and three vertical σ_v mirror planes containing the C_2 axes. One of the horizontal C_2 axes corresponds to the *pseudo*-two-fold axis for the entire cluster (minus the phosphorus-attached *p*-Tolyl substituents).

The view in Figure 1a portrays the Pd_{23} kernel along the principal three-fold axis passing through Pd(10) and Pd(11) with the perpendicular molecular C_2 axis that passes through Pd(1), being oriented vertically.

The strongly bonded $Pd(i)_3$ isosceles triangle in **1**, consisting of two shorter equivalent edges of 2.581(1) and 2.591(1) Å versus the third longer edge of 2.667(1) Å, is evidenced by the unusually short Pd(i)−Pd(i) mean of 2.61 Å; its deformation from an equilateral triangle is readily attributed to the pseudo-C_2 molecular distortion imposed on the Pd_{23} kernel by the additional capping Pd atoms (*vide infra*). Similarly short means were found for the six tetrahedral Pd(i)−Pd(i) edges (mean 2.56 Å; range, 2.537(2)−2.578(2) Å) within the Pd_{26} kernel in **2** and for the nine trigonal bipyramidal Pd(i)−Pd(i) edges (mean, 2.64 Å; range, 2.597(4)−2.664(4) Å) within the Pd_{29} kernel in **3**. Although the 12 individual radial Pd(i)−Pd(icosahedral) connectivities varied considerably with similar dispersions of 0.2−0.3 Å in each icosahedron within the kernels in **1**, **2**, and **3**,[5] their corresponding means are virtually identical: namely, 2.70−2.73 Å range within the Pd_{23} kernel in **1** versus 2.69−2.71 Å range within the Pd_{26} kernel in **2** and 2.72−2.73 Å range within the Pd_{29} kernel in **3**. Likewise, the tangential Pd(cage)−Pd(cage) means (2.85−2.88 Å) and their dispersions (2.6−3.4 Å) are almost identical for the three icosahedra in **1**. As previously found in **2** and **3**, the experimentally determined radial compression of 5.2% {i.e., [(2.87 Å − 2.72 Å)/2.87 Å] × 100} is in agreement with the predicted value of ca. 5% for a geometrically regular centered icosahedron.[15]

(15) Mackay, A. L. *Acta Crystallogr.* **1962**, *15*, 916.

Table 1. Mean Connectivities and Corresponding Individual Ranges for $Pd_{37}(CO)_{28}\{P(p\text{-Tolyl})_3\}_{12}$ (**1**) Possessing *pseudo-C_2* Symmetry

connectivity[a]		N^e	mean (Å)	range (Å)
	Pd(i)−Pd(i)	2	2.59	2.581(1)−2.591(1)
		1	2.67	2.667(1)
icosahedron with Pd(1) center:	Pd(i)−Pd(cage)	12	2.70	2.581(1)−2.801(1)
	Pd(cage)−Pd(cage)	30	2.85	2.667(1)−3.207(1)
icosahedron with Pd(2) center:	Pd(i)−Pd(cage)	12	2.73	2.581(1)−2.908(1)
	Pd(cage)−Pd(cage)	30	2.87	2.591(1)−3.338(1)
icosahedron with Pd(3) center:	Pd(i)−Pd(cage)	12	2.73	2.591(1)−2.898(1)
	Pd(cage)−Pd(cage)	30	2.88	2.581(1)−3.358(1)
Pd(j)−Pd(cage), where Pd(j) is Pd(24)/Pd(25)		6	2.84	2.682(1)−3.120(1)
Pd(j)−Pd(cap), where Pd(j) is Pd(24)/Pd(25)		6	2.79	2.682(1)−2.865(1)
Pd(cap)−Pd(cage), where Pd(cap) are regular triangular-face condensed Pd(33)/Pd(36)		6	2.74	2.693(1)−2.763(1)
Pd(cap)−Pd(cage), where Pd(cap) are near-regular triangular-face condensed Pd(34)/Pd(35)		6	2.78	2.680(1)−2.929(1)
Pd(cap)−Pd(cage), where Pd(cap) are non-regular triangular-face condensed Pd(26)/Pd(37)		6	2.93	2.699(1)−3.479(1)
Pd(cap)−Pd,[b] where Pd(cap) are non-regular triangular-face condensed Pd(30)/Pd(31)		6	2.87	2.682(1)−3.209(1)
Pd(cap)−Pd,[c] where Pd(cap) are five-metal coordinated Pd(28)/Pd(29)		10	2.82	2.709(1)−2.978(1)
Pd(cap)−Pd,[d] where Pd(cap) are five-metal coordinated Pd(27)/Pd(32)		10	2.88	2.708(1)−3.209(1)
Pd(cap)−Pd(cap), where pairs are Pd(27)−Pd(31), Pd(30)−Pd(32)		2	3.19	3.163(1)−3.209(1)
	Pd−P	12	2.32	2.295(2)−2.338(2)
	Pd−(μ_2-CO)	44	2.03	1.915(7)−2.111(6)
	Pd−(μ_3-CO)	18	2.12	2.036(6)−2.211(7)

[a] Pd(i) denotes three triangular interior atoms ($n = 1-3$); Pd(cage) denotes the 20 icosahedral cage atoms ($n = 4-23$) for the three interpenetrating DI; Pd(j) denotes the two P-free Pd(24), Pd(25) atoms; and Pd(cap) denotes the 12 capping atoms ($n = 26-37$) with P-ligands. [b] Pd denotes three different Pd(cage), Pd(j), and Pd(cap) atoms. [c] Pd denotes four Pd(cage) and one Pd(j) atoms. [d] Pd denotes three Pd(cage), one Pd(j), and one Pd(cap) atoms. [e] Designates the total number of individual connectivities for a given mean.

Figure 1b displays the same view (as shown in Figure 1a) of the geometrical arrangement about the Pd(n) kernel ($n = 1-23$) of the 14 other Pd(n) atoms ($n = 24-37$), which lower the *pseudo*-symmetry of the entire Pd$_{37}$ core from D_{3h} to C_2. These dark-green colored capping atoms consist of two phosphorus-free Pd(24)/Pd(25) atoms, labeled Pd(j) in Table 1, and 12 P(p-C$_6$H$_4$Me)$_3$-ligated Pd(cap) atoms. They display a remarkable diversity of asymmetrical coordination modes with the Pd(cage) atoms as well as with one another. Table 1 lists the different types of the resulting Pd−Pd connectivities, which vary over a wide range from 2.7 to 3.5 Å for these 14 capping atoms that are classified in pairs under the molecular *pseudo-C_2* symmetry.

c. P(p-Tolyl)$_3$/CO Ligation. The highly non-spheroidal Pd$_{37}$ architecture is stabilized by 12 P(p-C$_6$H$_4$Me)$_3$ and 28 bridging carbonyl ligands that form a protective coating about the Pd$_{37}$ core (see Figure 1b,c). As evidenced from these figures, the 12 Pd(cap)-attached P atoms closely adhere to molecular *pseudo-C_2* symmetry. The average Pd−P distance (mean, 2.32 Å; range, 2.295(2)−2.338(2) Å) is analogous with those of 2.29 and 2.31 Å in the trimethylphosphine-ligated **2** containing the Pd$_{26}$ kernel and **3** containing the Pd$_{29}$ kernel, respectively.

Figure 1c displays the steric dispositions of the 22 doubly bridging and 6 triply bridging carbonyl ligands, whose connectivities also conform to the *pseudo-C_2* symmetry. Each of the eight triangular capping Pd(cap) atoms has two doubly bridging COs that connect these atoms either to two icosahedral Pd(cage) atoms or, in the case of the C_2-related Pd(30), Pd(31) atoms, to one Pd(cage) and one phosphorus-free Pd(j) atom. Each of the other four five-metal coordinated Pd(cap) atoms (see Table 1) is connected by one doubly bridging CO to one Pd(cage) atom and by one triply bridging CO to another Pd(cage) atom and one Pd(j) atom. The remaining two doubly bridging C(n)O(n) ligands ($n = 4, 21$) and two triply bridging C(n)O(n) ligands ($n = 7, 11$) are linked only to icosahedral Pd(cage) atoms. As expected, Pd−Pd bonding connectivities also linked by bridging

carbonyl ligands are generally observed to be markedly shorter (i.e., in the 2.7−2.8 Å Pd−Pd range) relative to non-CO-bridged ones.

Direct Analogy of 23-, 26-, and 29-Atom II Pd Kernels of DI Units with Corresponding DI Models for Charged Argon Clusters and Resulting Implications. A growth-sequence cluster model of interpenetrating icosahedra (II) composed of 19-atom double icosahedra (DI), each formed from two interpenetrating 13-atom centered icosahedra sharing seven common atoms, was presented by Farges and co-workers[13a] in 1985. Their particular atomic growth pattern from an original 13-atom centered icosahedron involved the geometrical atom-by-atom construction of the maximum number of possible DI units within a given II in order to achieve maximization of nearest-neighbor connectivities. Their constructed family of DI models included the following members: (1) 19-atom D_{5h} linear model composed of two II (with one DI along interior bonding line); (2) 23-atom D_{3h} trigonal-planar model composed of three II (with three DI along three interior triangular bonding edges); (3) 26-atom T_d tetrahedral model of four II (with six DI along six interior tetrahedral bonding edges); and (4) 29-atom D_{3h} trigonal-bipyramidal model of five II (with nine DI along nine interior trigonal-bipyramidal bonding edges). Of prime interest is that Farges et al.[13a] pointed out that their 23-atom model possessing three DI (observed in **1**) was found only in their particular II growth sequence, in contrast with their other formulated n-atom models having been previously postulated in other growth sequences. Furthermore, they showed that their particular n-atom DI models (with $n = 19, 23, 26, 29$) possess higher binding energies per atom than those for other similar size models.[16] In a further comprehensive analysis in 1988, Farges et al.[13b]

(16) (a) Hoare, M. R.; Pal, P. *Adv. Phys.* **1971**, *20*, 161. (b) Hoare, M. R.; Pal, P. *Adv. Phys.* **1975**, *24*, 645. (c) Briant, C. L.; Burton, J. J. *Phys. Status Solidi B* **1978**, *85*, 393.
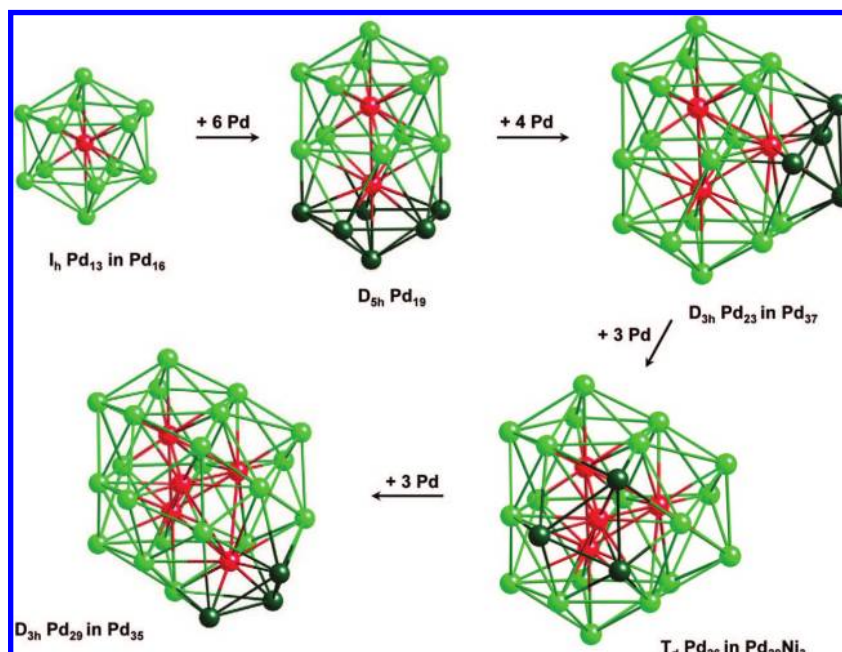
Figure 2. Possible sequential growth transformations for generation of the interpenetrating icosahedral (II) Pd$_n$ family of double icosahedra (DI) units from a 13-atom centered Pd$_{13}$ icosahedron [found in Pd$_{16}$(CO)$_{13}$(PR$_3$)$_9$ (R = Me, Et)] to the central 29-atom centered Pd$_{29}$ pentaicosahedral kernel (5II, 9DI). The centered 23-atom *pseudo-D$_{3h}$* Pd$_{23}$ kernel (found in **1**) consists of three II forming three trigonal planar DI units that are oriented along the three bonding edges of the centered interior *pseudo*-equilateral Pd$_3$ triangle. This non-*spheroidal* Pd$_{23}$ kernel may transform into the central 26-atom *pseudo-T$_d$ spheroidal* Pd$_{26}$ kernel (found in **2**), which is composed of *four* II forming *six* DI units that are oriented along the *six* binding edges of the central interior Pd$_4$ tetrahedron; in turn, a further transformation gives rise to the central 29-atom *pseudo-D$_{3h}$* Pd$_{29}$ kernel (found in **3**), composed of five II forming *nine* DI units that are oriented along the *nine* bonding edges of the central interior Pd$_5$ trigonal bipyramid. These transformations are presumed to be controlled by the steric effects of the phosphine ligands as well as by the resulting protective coating of the entire ligand polyhedron about the metal core.

established that the sequential growth pattern based upon their atomic structural DI models is in complete agreement with the strong atom-peak maxima at 19, 23, 26, and 29 (and higher) observed in the mass spectrum reported by Harris et al.[14] in 1984 of charged argon clusters generated in a low-temperature free-jet expansion.

We propose the same growth sequence (Figure 2) in the sequential construction of the *n*-atom II Pd$_n$ kernels (*n* = 19, 23, 26, 29) from the 13-atom centered icosahedron.[17−21] This pattern is based upon the maximization of nearest-neighbor connectivities during the construction of the adjacent higher *n*-atom member of the DI family via the addition of Pd atoms on certain adjacent faces. This resulting growth pattern (given in Figure 2) of II composed of 19-atom DI, with the icosahedral-centered interior atoms forming strong bonding connectivities, is visualized in Figure 3, in which each 13-atom centered icosahedron is symbolized as a centered sphere.
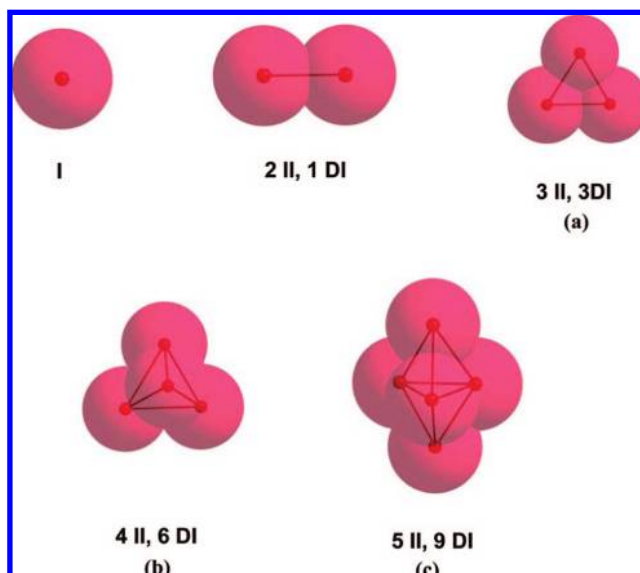
(17) The classic *D$_{5h}$* Pt$_{19}$ core in the [Pt$_{19}$(CO)$_{22}$]$^{4-}$ tetra-anion[18] may be viewed as a conformational isomer of the 19-atom *D$_{5h}$* II model (1 DI), for which the three pentagonal Pt$_5$ rings are constrained to be eclipsed instead of staggered due to the 10 doubly bridging COs linking eclipsed pairs of Pt atoms between pentagonal rings.

(18) Washecheck, D. M.; Wucherer, E. G.; Dahl, L. F.; Ceriotti, A.; Longoni, G.; Manassero, M.; Sansoni, M.; Chini, P. *J. Am. Chem. Soc.* **1979**, *101*, 6110.

(19) Recent X-ray crystallographic studies[20] revealed that the Au$_{12}$Ag$_7$ and Au$_{17}$Ag$_2$ skeletons in Au$_{12}$Ag$_7$(PMe$_2$Ph)$_{10}$(NO$_3$)$_9$ (**1**) and Au$_{17}$Ag$_2$-(PMe$_2$Ph)$_{10}$(NO$_3$)$_9$ (**2**), respectively, both form a 19-atom interpenetrating bi-icosahedral polyhedron (2 II; 1 DI) of *D$_{5h}$* symmetry. Their ordered bimetallic cores consist of two outer eclipsed Ag-capped Au$_5$ pentagons that each form Au-centered icosahedral cages with a staggered inner Ag$_5$ pentagon in **1** that is replaced by a Au$_5$ pentagon in **2**.

(20) Nunokawa, K.; Ito, M.; Sunahara, T.; Onaka, S.; Chiba, H.; Funahashi, Y.; Masuda, H.; Yonezawa, T.; Nishihara, H.; Nakamoto, M.; Yamamoto, M. *Dalton Trans.* **2005**, 2726.

Figure 3. Conceptual view of the sequential growth process of interpenetrating icosahedra (II) composed of 19-atom double icosahedra (DI) to give the 19-, 23-, 26-, and 29-atom family members from a centered icosahedron designated by a centered sphere.

This remarkable unparalleled analogy between the formation and stabilization of geometrically identical idealized architectures for the three II Pd kernels with corresponding DI models constructed for the generated charged argon clusters gives rise to two highly significant stereochemical implications: (1) it provides compelling evidence that the nature of delocalized Pd−Pd bonding in these II (and presumably other nanosized) Pd clusters, in which each zerovalent Pd atom individually

possesses a closed-subshell $4d^{10}$ ground state, may analogously (as in argon clusters) be viewed primarily in terms of (considerably stronger) *attractive dispersion interactions*;[21] (2) the geometrical conformity of the II Pd_{23} kernel of 3DI in **1** to the 23-atom D_{3h} trigonal-planar model (3II, 3DI) found only in the growth sequence put forth by Farges et al.[13] is especially important in furnishing experimental evidence that the central *pseudo-D_{3h}* tetrahedral Pd_{26} kernel (4II, 6DI) in the PMe_3-ligated $Pd_{29}Ni_3(CO)_{22}(PMe_3)_{13}$ (**2**) and the central *pseudo-D_{3h}* trigonal-bipyramidal Pd_{29} kernel (5 II, 9 DI) in the PMe_3-ligated $Pd_{35}(CO)_{23}P(Me_3)_{15}$ (**3**) may similarly be generated via the same sequential growth pattern with the 23-atom palladium kernel functioning as an intermediate. In **1** the 12 bulky $P(p\text{-}Tolyl)_3$ ligands (Tolman[8] cone angle, 145°) found about the entire Pd_{37} core sterically necessitate the observed *extended* metal surface, which originates from its *pseudo*-2D trigonal-planar Pd_{23} kernel. The *ligand-induced* buildup of the Pd_{23} kernel to Pd_{37} thereby prevents its *alternative* conversion into a *spheroidal* tetrahedral II Pd_{26} kernel. On the other hand, the much smaller PMe_3 ligands (Tolman[8] cone angle, 118°) found in **2** and **3** have minimal steric effects that would allow further sequential transformations of an initially generated 23-atom II intermediate palladium kernel into the 26-atom *spheroidal* II palladium kernel in **2** or further into the 29-atom *semi-spheroidal* II palladium kernel in **3**, but yet with smaller total metal-core nuclearities of 32 and 35, respectively.[21]

A comprehensive density functional theory (DFT) investigation, which utilized the TURBOMOLE program package, was reported in 2003 by Nava, Sierka, and Ahlrichs[22] on neutral, ligand-free palladium architectures which included several from our published ligand-stabilized icosahedral palladium clusters: namely, the centered Pd_{13} icosahedron of $Pd_{16}(CO)_{13}(PMe_3)_9$,[5] the 26-atom four II and 29-atom five II kernels found in **2** and **3**, respectively, the mixed face-fused icosahedral/octahedral Pd_{29} kernel of $Pd_{59}(CO)_{32}(PMe_3)_{21}$,[5] and the capped 145-atom three-shell palladium core of $Pd_{145}(CO)_x(PEt_3)_{30}$ ($x \sim 60$).[6] The calculations reported in ref 22 showed that the "bare" II Pd_n intermediates ($n = 19, 23, 26$) formed in our proposed sequential growth pathway from the Pd_{13} icosahedron to the Pd_{29} kernel were *not* due to the energetics of the "naked" Pd_n clusters, in that they often were appreciably less stable than alternative close-packed structures. Hence, Ahlrichs and co-workers[22] concluded that "ligand and kinetic effects may play an important role in driving the formation of ligand-stabilized clusters." The

same conclusion was emphasized in analogous calculations on the "bare" icosahedral uncapped three-shell Pd_{115} architecture and corresponding "bare" (30-atom)-capped architecture of the Pd_{145} cluster. The fact that their calculated cohesive energies were remarkably lower than those of other clusters of similar sizes led to their conclusion that "ligands must play an important role in stabilizing the cluster cores."

The above conclusions by Ahlrichs and co-workers[22] from DFT calculations on ligand-free ("naked") metal cores of our icosahedral-based palladium clusters are completely consistent with our view that the formation of each cluster involves the prior assembly by an organized synthetic route of a certain icosahedral-based central kernel, which itself is presumably constructed from coordinatively unsaturated ligated palladium fragments; generation of the entire palladium cluster may then involve the *concomitant* stabilization of the partially ligated kernel with additional ligands and capping ligated palladium atoms (commonly kinetically controlled) in order to satisfy electronic/steric effects. We previously have emphasized that the unique tendency of palladium among the Group 8–10 transition metals to generate a large variety of ligated nanosized clusters with geometrically unprecedented icosahedral-based metal frameworks may be ascribed to palladium metal possessing the lowest cohesive energy (i.e., weakest metal–metal bonding).

Other Icosahedral-Based Nanosized Clusters and Resulting Implications. A single centered icosahedral Pd_{13} kernel of *pseudo-I_h* symmetry was found in the isostructural $Pd_{16}(CO)_{13}(PR_3)_9$ clusters (R = Me,[5] Et[23]), in which three additional exopolyhedral triangular-planar $Pd(\mu_2\text{-}CO)_2PR_3$ fragments edge-bridge the Pd_{13} icosahedron.

A totally dissimilar type of tri-icosahedral-based nanosized $Pd_n(CO)_x(PR_3)_y$ cluster is exemplified by $Pd_{69}(CO)_{36}(PEt_3)_{18}$,[24] which contains a linear 33-atom faced-sharing Pd_{33} tri-icosahedron of *pseudo-D_{3d}* symmetry that is formally constructed via face condensations of two outer centered icosahedra on centrosymmetrically opposite triangular faces of the inner centered icosahedron. This so-called tri-icosahedral Pd_{33} kernel in the Pd_{69} cluster may be considered as a permanent guest residing inside a hexagonal-shaped Pd_{30} tube formed by cyclic *trans* edge-sharing of six Pd_7-centered hexagons (host).

A completely different vertex-sharing icosahedral growth sequence is observed for centered polyicosahedral Au–Ag and Au–Ag–M halide phosphine superclusters (where M = Ni, Pd, Pt are centered M atoms). These extraordinary coinage-metal polyicosahedral clusters were prepared by Teo, Zhang, and co-workers,[25] who formulated a vertex-fused sequence of modular centered icosahedral building blocks to account for the formation of known and proposed polyicosahedral geometries. One of the known examples is a crystallographically analyzed 36-atom tri-icosahedral Au–Ag chloride $P(p\text{-}Tolyl)_3$ cluster, $Au_{18}Ag_{20}\{P(p\text{-}Tolyl)_3\}_{12}Cl_{14}$,[26] consisting of three Au-centered icosahedra sharing three vertices in a cyclic array; this particular $Au_{18}Ag_{18}$ tri-icosahedron was found to possess two additional exopolyhedral capping Ag atoms located on the idealized threefold axis. An alternative interpretation of the closed-shell requirements of these vertex-linked polyicosahedra has been put forth by Mingos and co-workers.[27]

(21) Based upon only crystallographic examples of the 26- and 29-atom II Pd kernels previously uncovered in the crystal structure determinations[5] of **2** and **3**, respectively, the same sequential II growth pathway and subsequent postulation concerning Pd–Pd bonding in these ligated palladium clusters being attributed primarily to *attractive dispersion forces* were initially postulated[5] in 2001. The isolation, structural analysis, and resulting implications of the 23-atom II kernel in **1** (reported herein) furnish additional self-consistent "strong" support in favor of these experimentally based proposals, which indicate that palladium is the only known Group 8–10 transition metal that can simulate argon atoms in forming analogous icosahedral-based clusters.

(22) Nava, P.; Sierka, M.; Ahlrichs, R. *J. Phys. Chem. Chem. Phys.* **2003**, *5*, 3372.

(23) Mednikov, E. G.; Slovokhotov, Yu. L.; Struchkov, Yu. T. *Metalloorg. Khim.* **1991**, *4*, 123; *Organomet. Chem. USSR* **1991**, *4*, 65 (Engl. transl.)

(24) Tran, N. T.; Dahl, L. F. *Angew. Chem., Int. Ed.* **2003**, *42*, 3533.

(25) (a) Teo, B. K.; Zhang, H.; Shi, X. *J. Am. Chem. Soc.* **1990**, *112*, 8552. (b) Teo, B. K.; Zhang, H. *Proc. Natl. Acad. Sci. U.S.A.* **1991**, *88*, 5067, and references therein. (c) Teo, B. K.; Zhang, H. *Coord. Chem. Rev.* **1995**, *143*, 611. (d) Teo, B. K.; Zhang, H. *Inorg. Chim. Acta* **1997**, *265*, 213. (e) Teo, B. K.; Strizhev, A.; Elber, R.; Zhang, H. *Inorg. Chem.* **1998**, *37*, 2482.

(26) (a) Teo, B. K.; Hong, M.; Zhang, H.; Huang, D.; Shi, X. *J. Chem. Soc., Chem. Commun.* **1998**, 204. (b) Teo, B. K.; Zhang, H.; Shi, X. *J. Am. Chem. Soc.* **1990**, *112*, 8552.

(27) Lin, Z.; Kanters, R. P. F.; Mingos, D. M. P. *Inorg. Chem.* **1991**, *30*, 91.

Condensations of centered icosahedra that produce either the 23-atom interpenetrating tri-icosahedral Pd$_{23}$ kernel (composed of three DI), which may further transform into Pd$_{26}$ or Pd$_{29}$ kernels, or the 33-atom faced-fused tri-icosahedral Pd$_{33}$ kernel in the above-mentioned Pd$_{69}$ cluster emphasize that similar condensation growth processes presumably occur in the formation of unligated and ligated nanoparticles. One may conclude that the existence of different kinds of ligated icosahedral-based metal clusters is dependent upon the cohesive energies and relative electronegativities of the metal atoms, electronic/steric effects of their ligands, and the interplay of kinetic and thermodynamic effects, as dictated by the reaction boundary conditions.

Synthesis and Spectroscopic Characterization of 1: Dissimilar Major Cluster Product Isolated from Thermolysis Reaction of Analogous Pd$_{10}$(CO)$_{12}$(PR$_3$)$_6$ Precursor upon PPh$_3$-for-P(p-Tolyl)$_3$ Ligand Substitution. The synthesis of **1** is based on the well-established ability of CO/PR$_3$-ligated Pd$_{10}$ clusters to undergo enlargement under inert atmosphere and moderately elevated temperatures. Accordingly, **1** was prepared from Pd$_{10}$(CO)$_{12}$[P(p-Tol)$_3$]$_6$[12] via short-time heating in THF solution. Both its stoichiometry and atomic arrangement were unequivocally established from a low-temperature (100 K) CCD X-ray diffractometry study. The calculated Pd/P atom % ratio (37Pd/12P) of 75.5%/24.5% is in reasonable agreement with those of 76.4%/21.9% and 77.5%/21.5% obtained from energy-resolved measurements on two crystals with a field emission scanning electron microscope. An IR spectrum of **1** (Nujol) revealed bridging carbonyl bands in the range of 1900−1850 cm^{-1}, which are consistent with the solid-state structure. A ^{31}P{^{1}H} NMR spectrum in CD$_2$Cl$_2$ solution at room temperature showed at least five signals, four of which were broadened. The number, relative intensities, and shapes of these signals could not be interpreted in a clear-cut way.

It was of particular interest to investigate the effect of PPh$_3$-for-P(p-Tolyl)$_3$ ligand substitution in the parent Pd$_{10}$ precursor on the metal nuclearity and composition/shape of cluster product(s). Both ligands have identical steric (shielding) properties (same Tolman[8] cone angle, 145°); the greater electron-donating ability of the P(p-Tolyl)$_3$ ligand is in accordance with its basicity (pK_a = 3.84) being 1 order of magnitude larger than that of PPh$_3$ (pK_a =2.73),[28] as well as illustrated indirectly by the lower carbonyl frequency of 2066.7 cm^{-1} in the tetrahedrally coordinated Ni(CO)$_3$P(p-Tolyl)$_3$ compared to that of 2068.9 cm^{-1} in the structurally analogous Ni(CO)$_3$PPh$_3$ complex.[8]

The immediately formed product of the thermolysis of Pd$_{10}$(CO)$_{12}$(PPh$_3$)$_6$ in THF solution (65 °C, 30−35 min, N$_2$) was determined *not* to be the PPh$_3$-ligated Pd$_{37}$ analogue of **1** but instead the known Pd$_{12}$(CO)$_{12}$(PPh$_3$)$_6$,[9b] which has a hexacapped octahedral Pd$_{12}$ core. In addition, the same procedure used for the preparation of **1** also afforded two types of crystals, namely needles and hexagonal plates, that were isolated and characterized by IR spectra; neither crystal type produced suitable X-ray diffraction data for crystallographic analysis. The formation of Pd$_{12}$(CO)$_{12}$(PPh$_3$)$_6$ as a straightforward dissimilar product is not surprising. In fact, this cluster, which is *insoluble in organic solvents*, was prepared with considerable yields (67%−84%) from two precursors, Pd$_4$ and Pd$_{10}$, under different reaction conditions.[9c] Therefore, the formation of the PPh$_3$-ligated Pd$_{12}$ cluster cannot be ascribed only to the weaker electron-donating ability of the PPh$_3$ ligand versus that of P(p-

Tolyl)$_3$. The generally smaller solubilities of PPh$_3$ derivatives are also presumed to have an important effect on solution lifetimes of intermediates and, in this way, may alter the product composition.

Electron-Counting Analysis of 1. The observed number of cluster valence electrons in **1** is 450 electrons [(37 × 10)(Pd) + (28 × 2)(CO) + (12 × 2)(P(p-Tol)$_3$) = 450]. Because previous applications[5] of the Mingos condensation rules[29] successfully accounted for the different atom-type capping condensations of the Pd$_{26}$ and Pd$_{29}$ kernels of **2** and **3**, respectively, **1** was likewise considered in terms of face condensations by capping atoms of its Pd$_{23}$ tri-icosahedral kernel. Based upon this kernel having an interior Pd(i)$_3$ triangle (Δ$_i$ = 48 electrons) that is encapsulated by 20 surface Pd(cage) atoms (n_s = 20), the resulting electron count for the Pd$_{23}$ kernel is 288 electrons [viz., Δ$_i$ + 12n_s = 48 + (12 × 20) = 288].

The Mingos condensation rules[29] applied under *pseudo-C$_2$* molecular symmetry give rise to additional electron counts for the following face-condensation patterns (see Figure 1a,b). (a) Six tetrahedra, each composed of one Pd(cap) and three Pd(cage) atoms, formed under C_2 symmetry by three pairs of Pd(cap) atoms (n = 33/36, 34/35, 26/37). The resulting electron count, based upon the condensation of a tetrahedron onto the Pd$_{23}$ kernel through a common triangular Pd(cage) face, is 6 × (60 − 48) = 72 electrons. (b) Two trigonal bipyramids, each composed of one Pd(cap) and four Pd(cage) atoms, that are formed from the two C_2-related Pd(n) capping atoms (n = 28/29). This pattern involves the condensation of each trigonal bipyramid (viz., 72 electrons) onto the Pd$_{23}$ kernel through two common edge-sharing "butterfly" triangles [viz., (2 × 48) − 34 = 62 electrons], resulting in an electron count of 2 × (72 − 62) = 20 electrons. (c) Two six-atom monocapped trigonal bipyramids (MTBs), each composed from three Pd(cage), one Pd(j), and two Pd(cap) atoms. These two MTBs, consisting under C_2 symmetry of Pd(14/21, 18/20, 19/23)$_{cage}$Pd(24/25)$_j$Pd(27/32, 31/30)$_{cap}$ atoms, are condensed onto the Pd$_{23}$ kernel through corresponding common triangular Pd(cage) faces. Pd(n) atoms occupy the vertices of each MTB as follows: three (n = 14/21, 18/20, 27/32) are equatorial, two (n = 19/23, 24/25) apical, and one (n = 31/30) is the monocapped atom that caps the triangular face consisting of three common atoms (n = 18/20, 24/25, 27/32). This assemblage results in an electron count of 72 electrons [viz., 2 × (72 + 60 − 48 − 48) = 72). The total calculated electron count of 452 electrons (viz., 288 + 72 + 20 + 72 = 452) is two electrons more than the observed number of 450 electrons for **1**. However, the condensation pattern of at least one pair of Pd(n) atoms (viz., n = 26/37) may be considered as edge-bridged instead of face-condensed due to the third Pd−Pd connectivity being significantly longer than the two others: namely, the longer 3.26 Å versus two shorter identical Pd−Pd distances of 2.71 Å for Pd(26), and the longer 3.48 Å versus two shorter Pd−Pd distances of 2.70 and 2.72 Å for Pd(37). Because the electron count for two edge-bridged Pd(n) atoms

(28) Allman, T.; Goel, R. G. *Can. J. Chem.* **1982**, *60*, 716.

(29) (a) Mingos, D. M. P. *Acc. Chem. Res.* **1984**, *17*, 311. (b) Mingos, D. M. P. *Polyhedron* **1984**, *3*, 1289. (c) Hall, K. P.; Mingos, D. M. P. *Prog. Inorg. Chem.* **1984**, *32*, 237. (d) Mingos, D. M. P.; Johnson, R. L. *J. Organomet. Chem.* **1985**, *281*, 419. (e) Mingos, D. M. P.; Zhenyang, L. *J. Chem. Soc., Dalton Trans.* **1988**, 1657, and references therein. (f) Mingos, D. M. P.; May, A. P. In *The Chemistry of Metal Cluster Complexes*; Shriver, D. F., Kaesz, H. D., Adams, R. D., Eds.; VCH Publishers: New York, 1990; Chapter 2, pp 11−119. (g) Mingos, D. M. P.; Wales, D. J. *Introduction to Cluster Chemistry*; Prentice Hall: Old Tappan, NJ, 1990. (h) Mingos, D. M. P.; Watson, M. J. *Adv. Inorg. Chem.* **1992**, *39*, 327.

(two condensed triangles) is $2 \times (48 - 34) = 28$ instead of 24 for two face-condensed atoms (two condensed tetrahedra), the total number of electrons for **1** is then 456.

The same total electron count of 456 electrons is obtained for **1** from more general applications of markedly different models for metal clusters assumed to possess close-packed core geometries. These include the following: (1) the Mingos model,[29] given by $\Delta_i + 12n_s$, where $\Delta_i = 48$ for an encapsulated metal triangle and $n_s = 34$ for the other 34 surface atoms [viz., $48 + (12 \times 34) = 456$]; (2) the Teo/Zhang model,[30] given by $2(6G + K)$, where G denotes the total number of metal atoms (viz., 37) and $K = 6$ for a triangle centered at a hole [viz., $2((6 \times 37) + 6) = 456$]; and (3) the Ciani/Sironi approach,[31] involving the number of cluster valence molecular orbitals, given by $6N_M + X$, with the free variable X (of range 6−11) assumed in this case to have the lowest value of 6 [viz., $2((6 \times 37) + 6) = 456$].

In sharp contrast, the PMe$_3$-ligated Pd$_{29}$Ni$_3$(CO)$_{22}$(PMe$_3$)$_{13}$ (**2**) and Pd$_{35}$(CO)$_{23}$(PMe$_3$)$_{15}$ **3** containing the *quasi*-spheroidal Pd$_{26}$ and Pd$_{29}$ kernels, respectively, possess much more regular metal-core arrangements (*vide supra*), and thereby their observed electron counts conform exactly to the straightforward application[5] of the analogous Mingos condensation rules. It is apparent that the above variation in the number of calculated cluster electrons in **1** (namely, 450 electrons versus 456 electrons) obtained by application of different models is a consequence of the highly irregular non-spheroidal structure that makes it difficult to account for the highly asymmetrical condensation modes of the Pd(j) and Pd(cap) atoms onto the Pd$_{23}$ kernel. Consequently, there appears to be no appropriate electron-counting approach that can furnish a reliable electron count for **1**.

Experimental Section

General Comments. Reactions were carried out via standard Schlenk techniques on a preparative vacuum line under a nitrogen atmosphere. Solvents were deoxygenated prior to their use by the purging of N$_2$ through them for at least 20 min at room temperature. Pd$_{10}$(CO)$_{12}$[P(*p*-Tol)$_3$]$_6$ and Pd$_{10}$(CO)$_{12}$(PPh$_3$)$_6$ were prepared in accordance with literature procedures[12] and used without additional purification. An ambient-temperature ^{31}P{^{1}H} NMR spectrum was obtained under N$_2$ atmosphere on a Bruker AC-300 spectrometer and referenced to 85% H$_3$PO$_4$ in D$_2$O as an external standard. Infrared spectra were recorded on a Mattson Polaris FT-IR spectrometer; Nujol mulls were prepared under nitrogen. X-ray Pd/P microanalyses were carried out by Dr. Richard Noll (Manager of the SEM Facility at the Materials Science Center, University of Wisconsin−Madison) on a LEO 1530 field emission scanning electron microscope with an energy dispersive detector.

Synthesis of Pd$_{37}$(CO)$_{28}$[P(*p*-Tol)$_3$]$_{12}$ (1). A red solution of Pd$_{10}$(CO)$_{12}$[P(*p*-Tol)$_3$]$_6$ (0.300 g, 0.0930 mmol) in 5 mL of THF was stirred at 65 °C for 30 min. The resulting dark brown solution was kept overnight at room temperature and then filtered and crystallized via layering with hexane, which afforded 124 mg (56%) of black crystals of Pd$_{37}$(CO)$_{28}$[P(*p*-Tol)$_3$]$_{12}$·THF·3C$_6$H$_{14}$.

IR spectrum (Nujol), ν(CO): 1895 (s), 1868 (sh), 1852 (m) cm^{-1}. ^{31}P{^{1}H} NMR spectrum in CD$_2$Cl$_2$ (121.4 MHz): $\delta_1 = 41.5$ ppm (s, br), $\delta_2 = 28.5$ ppm (s, br), $\delta_3 = 27.4$ ppm (s), $\delta_4 = 25.3$ ppm (s, br), $\delta_5 = 20.2$ (s, br) with intensity ratios of $\delta_1/\delta_2/\delta_3/\delta_4/\delta_5 \approx$ 1.0/0.9/1.5/1.5/1.7.

Thermolysis of Pd$_{10}$(CO)$_{12}$(PPh$_3$)$_6$. The preparative procedure was performed in the same way as described above for **1**. A solution of Pd$_{10}$(CO)$_{12}$(PPh$_3$)$_6$ (0.200 g, 0.0672 mmol) in 7−8 mL of THF

was stirred under N$_2$ at 65 °C for 30−35 min. The black precipitate, Pd$_{12}$(CO)$_{12}$(PPh$_3$)$_6$ (45 mg, 25%), was filtered, washed with THF, and dried under vacuum.

IR spectrum (Nujol), ν(CO): 1895 (sh), 1883 (s), 1832 (s), 1801 (m), 1790 (sh) cm^{-1}. The frequencies and relative intensities of this three-band bridging carbonyl pattern are in complete agreement with those characteristic of the known Pd$_{12}$(CO)$_{12}$(PPh$_3$)$_6$; the two negligible shoulder bands, which were not observed in crystalline samples of the Pd$_{12}$ cluster, can be easily attributed to contaminations.

Further crystallization from THF solution in the presence of mixed hexane/acetone (1/4 ratio) afforded ∼30 mg of druses of needles and ∼5 mg of hexagonal plates; both types of crystals were unsuitable for an X-ray diffraction study.

X-ray Crystallographic Determination. A block-shaped cut crystal of size $0.46 \times 0.30 \times 0.28$ mm^3 was used for data collection. Intensity data were collected over an entire reciprocal lattice sphere at 100(2) K with a Bruker SMART CCD-1000 area-detector system mounted on a Bruker P4 diffractometer with graphite-monochromated Mo Kα radiation from a standard sealed-tube generator. A multiscan absorption correction (SADABS) was applied [μ(Mo Kα) $= 2.311$ mm^{-1}; max/min transmission, 0.564/0.416]. The crystal structure was determined by combined use of direct methods/difference Fourier syntheses together with least-squares refinement (based on F^2) performed with SHELXTL.[32]

Pd$_{37}$(CO)$_{28}$\{P(*p*-C$_6$H$_4$CH$_3$)$_3$\}$_{12}$·C$_4$H$_8$O·3C$_6$H$_{14}$: $M = 8704.83$; triclinic; $P\bar{1}$; $a = 20.6439(5)$ Å, $b = 22.0806(5)$ Å, $c = 36.0579(8)$ Å, $\alpha = 96.80°$, $\beta = 90.34°$, $\gamma = 114.67°$, $V = 14802.4(6)$ Å^3; $Z = 2$, $\rho_{calcd} = 1.954$ Mg/m^3. Mo Kα data were collected via 0.3ω scans over a 2θ range of 3.62−56.60°. Full-matrix least-squares refinement (3260 parameters; 359 restraints) on 68 887 independent reflections converged at w$R_2(F^2) = 0.112$, with $R_1(F) = 0.044$ for $I > 2\sigma(I)$; GOF (on F^2) = 0.92; max/min residual electron density, 2.42/−1.09 e·Å^{-3}. A structural CIF/PLATON test carried out by the http://journals.iucr.org/services/cif/checking/checkform.html service is in accordance with our crystal structure determination. CCDC reference number is 694281.

The crystallographically independent chemical part of the unit cell consists of one entire Pd$_{37}$(CO)$_{28}$\{P(*p*-Tol)$_3$\}$_{12}$ molecule, one THF, and three solvated hexane molecules ($Z = 2$). All non-hydrogen atoms, except for the carbon atoms of five disordered *p*-Tolyl groups and three hexane molecules, were refined anisotropically. Distance restraints were applied to the three hexane molecules and a number of *p*-Tolyl groups. Restraints on isotropic/anisotropic displacement parameters were applied to the carbon atoms of solvated hexane molecules and some carbon atoms of the *p*-Tolyl substituents; atoms in the latter groups were also restrained to lie in a plane. Of the disordered *p*-C$_6$H$_4$CH$_3$ groups, two are attached to the P9 atom (with site occupancies of 0.53/0.47 and 0.50/0.50), two are attached to the P10 atom (with site occupancies of 0.62/0.38 and 0.55/0.45), and one is attached to the P12 atom (with site occupancies of 0.52/0.48). All hydrogen atoms and the carbon atoms of several aromatic rings were generated geometrically and refined as riding models. The highest residual positive peak of 5.40 e·Å^{-3} on the subsequent difference map was found in the proximity of six Pd atoms (Pd15, Pd16, Pd19, Pd23, Pd33, and Pd36) with Pd−Pd distances of 2.54−3.15 Å, which is typical for Pd−Pd connectivities. Therefore, this peak may be attributed to an additional Pd atom, for which an estimated/refined occupancy factor of 0.05 was obtained. This kind of superposition of

(30) (a) Teo, B. K.; Zhang, H. *Inorg. Chim. Acta* **1988**, *144*, 173. (b) Teo, B. K.; Zhang, H. *Polyhedron* **1990**, *9*, 1985.
(31) Ciani, G.; Sironi, A. *J. Organomet. Chem.* **1980**, *197*, 233.

(32) (a) All crystallographic software and sources of the scattering factors are contained in the SHELXTL program library: Sheldrick, G. *SHELXTL*, version 6.14; Bruker Analytical X-Ray Systems: Madison, WI, 2000−2003. (b) Müller, P.; Herbst-Irmer, R.; Spek, A. L.; Schneider, T. R.; Sawaya, M. R. In *Crystal Structure Refinement: A Crystallographer's Guide to SHELXL*; Müller, P., Ed.; International Union of Crystallography, Oxford University Press: Oxford, UK, 2006.
(33) (a) Tran, N. T.; Kawano, M.; Powell, D. R.; Dahl, L. F. *J. Am. Chem. Soc.* **1998**, *120*, 10986. (b) Mednikov, E. G.; Dahl, L. F., manuscript in preparation.

"complete" molecules with minor contributions of "incomplete" ones, usually containing "naked" Pd atoms (as the prominent electron-density peaks), has been observed in other homo/hetero-palladium CO/PR$_3$-ligated nanosized clusters, including the crystal structures of Pd$_{59}$(CO)$_{32}$(PMe$_3$)$_{21}$[33a] and Au$_2$Pd$_{28}$(CO)$_{26}$(PEt$_3$)$_{10}$.[33b]

Supporting Information Available: X-ray crystallographic data, in CIF format, for **1**. This material is available free of charge via the Internet at http://pubs.acs.org.

JA805679J